5th International Symposium on Three-Dimensional Electromagnetics
Sapporo, Japan, May 7–9, 2013

Efficient Three-Dimensional Time Domain TEM Simulation Using Finite Elements, a Nonlocal Boundary Condition, Multigrid, and Rational Krylov Subspace Methods

Martin Afanasjew[1], Ralph-Uwe Börner[2], Michael Eiermann[1], Oliver G. Ernst[1], and Klaus Spitzer[2]
[1]Institute of Numerical Analysis and Optimizaion, TU Bergakademie Freiberg, Germany
[2]Institute of Geophysics and Geoinformatics, TU Bergakademie Freiberg, Germany

SUMMARY

We present a numerical method for the simulation of transient electromagnetic fields (TEM) in arbitrary three-dimensional conductivity distributions. The focus lies on models with an isolating air half-space, a model class that is of great importance in many applications. Our method allows us to restrict the computational domain to the subsurface by modeling the effect of the air half-space in terms of a nonlocal boundary condition at the air-earth interface. The spatial discretization is done using the finite element method employing Nédélec elements on an unstructured tetrahedral grid. Rational Krylov subspace methods in conjunction with a geometric multigrid method are used on the resulting linear system of ODEs to advance an initial electric field to selected times of interest. We present a number of standard models. The obtained results clearly show the reduction in computational effort compared to previous implementations.

Keywords: finite element method, Krylov subspace, nonlocal boundary condition, time domain, transient EM

INTRODUCTION

The transient electromagnetic (TEM) method has become a standard technique in geophysical prospecting during the past years. It is already in wide use, e. g., for the exploration of important resources like hydrocarbons, groundwater and minerals. One important aspect here is a reliable and computationally efficient simulation of the decaying electromagnetic field, which can be leveraged to get a better understanding of field behavior in complicated real-world settings as well as a building block in inversion schemes, that ultimately aim at resolving arbitrary conductivity structures from only a few well-placed measurements.

The predominant forward modeling technique in the literature is the finite difference time domain (FDTD) method, that was already introduced by Yee (1966). An explicit time-stepping technique, that already dealt with an isolating air half-space, was developed by Oristaglio and Hohmann (1984) for the two-dimensional case and later refined by Wang and Hohmann (1993) for three dimensions. Like for other explicit time-stepping methods, the size of the time steps, that the described Du Fort-Frankel scheme can stably perform, depends on the grid spacing and the lowest conductivity. Although the resistive air is already eliminated, thousands of time steps have to be performed although only a few dozen solutions are necessary to describe the decaying field.

The approach taken here is based on a finite element discretization, which allows for greater flexibility when modeling complicated conductivity structures. High accuracy is obtained with less effort compared to graded tensor product grids used with finite differences. It also helps in the construction of an analytic boundary condition, avoiding a few drawbacks the implementation by Wang and Hohmann (1993) has. Contrary to the finite difference approach, the matrices resulting from the discretization are symmetric and, thus, allow for a wide range of efficient and state-of-the-art time integration techniques, which can exploit this property. One such family of time integrators is based on building a rational Krylov subspace and extracting approximations to the matrix exponential function from that space, thus evaluating the sought electric field directly at a given time.

THEORY

Governing Equations

Our governing equation derives from Maxwell's equations in the diffusive limit. We have already used the constitutive relations and eliminated the magnetic field. Thus, we write

$$\mu\sigma\partial_t \boldsymbol{e} + \nabla\times\nabla\times\boldsymbol{e} = -\mu\partial_t \boldsymbol{j}^e \tag{1}$$

with

$\boldsymbol{e} = \boldsymbol{e}(\boldsymbol{x}, t)$	the electric field,
$\mu = \mu_0$	the magnetic permeability,
$\sigma = \sigma(\boldsymbol{x})$	the electrical conductivity, and
$\boldsymbol{j}^e = \boldsymbol{j}^e(\boldsymbol{x}, t)$	the impressed source current density.

The computational domain Ω is assumed to be a parallelepiped with its top surface aligned with the air-earth

interface Γ_0 at $z = 0$ on which we impose a special nonlocal boundary condition (see the next subsection). On the remaining boundaries, that are below the surface and are denoted Γ_s, we impose a simple perfect conductor boundary condition.

Our objective is to compute the electric field $\boldsymbol{e}_i$ at times t_i for $i \in \{1, 2, \ldots, n\}$ given an initial field $\boldsymbol{e}_0$ at t_0. We use sources that are switched off at $t = 0$ and therefore the right hand side of (1) vanishes for $t > 0$.

With all this information our initial-boundary value problem reads as:

$$\left.\begin{aligned} \mu\sigma\partial_t \boldsymbol{e} + \nabla\times\nabla\times\boldsymbol{e} &= 0 && \text{in } \Omega \\ \boldsymbol{n}\times\boldsymbol{e} &= 0 && \text{on } \Gamma_s \\ \partial_z \boldsymbol{e} &= \mathcal{T}\boldsymbol{e} && \text{on } \Gamma_0 \\ \boldsymbol{e}(0) &= \boldsymbol{e}_0 && \text{at } t_0 \end{aligned}\right\}. \tag{2}$$

Air-Earth Interface

The boundary condition imposed on Γ_0 is of special interest. Assuming $\sigma = 0$ in the air and transforming the resulting problem into Fourier domain, we can construct an explicit representation of the electric field in the air half-space. From that we can establish a link between the electric field $\boldsymbol{e}$ and its spatial derivative $\partial_z\boldsymbol{e}$ on Γ_0 using a linear operator $\mathcal{T}$:

$$\partial_z \boldsymbol{e} = \mathcal{T}\boldsymbol{e}. \tag{3}$$

The details for two dimensions are described by Goldman, Hubans, Nicoletis, and Spitz (1986) and the slightly more involved three-dimensional case is discussed by Goldman, Joly, and Kern (1989).

Spatial Discretization

The discretization with finite elements is done in the usual way, namely by transforming (2) into variational form and then applying the Galerkin method to obtain a finite-dimensional formulation. We use Nédélec finite elements, as dictated by the underlying physics, on a tetrahedral mesh. The only nonstandard part is the bilinear form b arising from (3) after a few more transformations in the Fourier domain

$$b(\boldsymbol{\varphi}, \boldsymbol{\psi}) = \iint_{\Gamma_0^2} k(\boldsymbol{x}, \boldsymbol{y}) \left(\nabla\times\boldsymbol{\varphi}(\boldsymbol{x})\right) \left(\nabla\times\boldsymbol{\psi}(\boldsymbol{y})\right) \,\mathrm{d}\boldsymbol{x}\,\mathrm{d}\boldsymbol{y} \tag{4}$$

with the Laplace kernel

$$k(\boldsymbol{x}, \boldsymbol{y}) = \frac{1}{2\pi\,\|\boldsymbol{x} - \boldsymbol{y}\|}. \tag{5}$$

The discretization of this integral yields a dense block (due to the nonlocal nature of the boundary condition) in an otherwise sparse stiffness matrix K. Together with the mass matrix M we obtain a semidiscretization in space—a system of ordinary differential equations ($\boldsymbol{u}$ represents the electric field in the finite element basis):

$$M\partial_t \boldsymbol{u} = K\boldsymbol{u}. \tag{6}$$

Time Integration

With $A = M^{-1}K$, the ODE (6) could theoretically be solved by directly evaluating

$$\boldsymbol{u}(t_i) = \mathrm{e}^{(t_i - t_0)A}\,\boldsymbol{u}_0. \tag{7}$$

This would require forming the inverse of the mass matrix and the exponential of its product with the stiffness matrix, which is both prohibitively expensive.

However, with a rational Krylov subspace method it is possible to extract an approximation $\boldsymbol{u}_m(t_i) \approx \boldsymbol{u}(t_i)$ from an m-dimensional Krylov subspace in an efficient way. More precisely, an approximate solution can be extracted from a rational Krylov subspace defined as follows

$$\mathcal{Q}_m(A, \boldsymbol{u}_0) := q_{m-1}^{-1}(A)\,\mathcal{K}_m(A, \boldsymbol{u}_0) \tag{8}$$

with $\mathcal{K}_m(A, \boldsymbol{u}_0) = \left\{\boldsymbol{u}_0, A\boldsymbol{u}_0, A^2\boldsymbol{u}_0, \ldots, A^{m-1}\boldsymbol{u}_0\right\}$ and

$$q_{m-1}(z) = \prod_{j=1}^{m-1} (z - \xi_j)\,. \tag{9}$$

Such subspaces are constructed, e. g., with the rational Arnoldi method to obtain an orthonormal basis from which approximations $\boldsymbol{u}_m(t_i) \in \mathcal{Q}_m(A, \boldsymbol{u}_0)$ can be computed. The subspace can be constructed in such a way that all solutions (for different times) can be extracted from the same subspace. We have some liberty in choosing the poles ξ_j. Their number and value highly impact the quality of the approximations that can be extracted from the subspace. Luckily, there is a heuristic to determine good poles for the approximation of the exponential function, given a certain parameter interval (in our case the times we want to advance to) and accuracy requirements (Güttel, 2010).

Multigrid

The cost of the rational Krylov method is mostly dominated by m solutions of systems of linear equations related to the matrix A. The matrix in our particular case—after some rearrangement of the algorithm—has the structure $M + sK$ with $s \in \mathbb{R}$.

We use a geometric multigrid method specially adapted to Nédélec finite elements (Arnold, Falk, & Winther, 2000) to solve those systems, either directly or as a preconditioner for the conjugate gradient method. Both variants achieve a prescribed accuracy in an almost constant number of iterations, yielding near-optimal computational complexity (almost linear in the number of unknowns). We also solve using a sparse direct solver for comparison.

NUMERICAL RESULTS

All computations were carried out on a machine with four AMD Opteron 6136 octo cores, running at 2.4 GHz with a total of 256 GB of RAM. The algorithms were implemented in pure MATLAB code running under MATLAB 2009b/2012a, with some finite element related tasks (nothing time-critical) performed by COMSOL 3.5a, both running in a 64-bit Linux environment. To generate reproducible timings we restricted ourselves to one computational thread that was explicitly pinned to one of the cores.

Setup

For every model we have constructed a hierarchy of successively refined meshes. Our source was the vertical magnetic dipole of unit strength, located at the origin, i. e., at the center of the face that coincides with the air-earth interface. The meshes were constructed such that they are fine in the vicinity of the source and become coarser at a distance from the source. We integrated from 10^{-5} s to 10^{-2} s with 20 time steps per decade.

We constructed the rational Krylov subspace with a fixed shift of $\xi_i \approx 2 \times 10^5$. The resulting shifted systems of linear equations were either solved by using the sparse direct solver PARDISO or by iterating with the conjugate gradient method (CG) up to a relative residual of 10^{-7}, the latter being preconditioned by one V-cycle of the geometric multigrid with the Arnold-Falk-Winther smoother. The systems on the coarsest grid of the multigrid were solved using a Cholesky decomposition.

Homogeneous Half-Space

The first considered model, which is primarily interesting due to its simplicity and the availability of an analytic solution, is the homogeneous half-space. The modeled domain has an extent of 3100 m × 3100 m × 1550 m with $\sigma = 0.1\,\mathrm{S\,m^{-1}}$. A solution for an exemplary time is plotted in Figure 1.

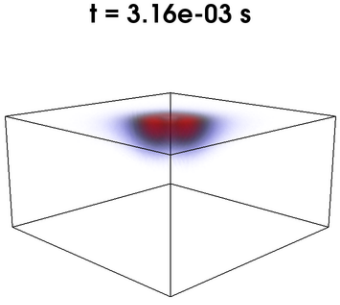

Figure 1. Normalized current densities of the homogeneous half-space model at $t \approx 3.2 \times 10^{-3}$ s.

Figure 2 compares solution times for different mesh sizes. While the sparse direct solver PARDISO is faster for smaller meshes, for bigger meshes it does not scale as well as CG with multigrid and has much higher memory requirements (not shown in the plot).

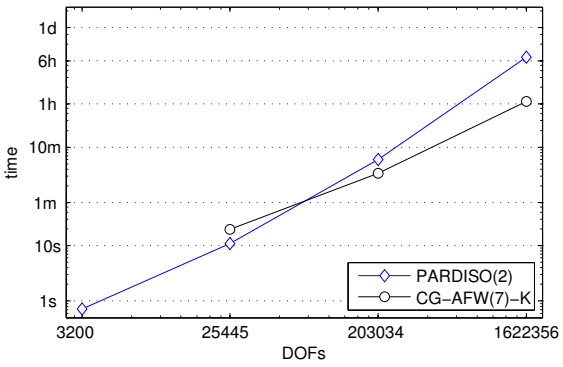

Figure 2. Computation times for the homogeneous half-space model for different grid sizes (identified by different number of degrees of freedom on the x-axis). The direct sparse solver PARDISO is compared to CG with multigrid as preconditioner.

Finally Figure 3 shows convergence results for a fixed time but varying size m of the Krylov subspace method. For the plotted time it can be seen that it would have been sufficient to construct a subspace of dimension ≈ 22 to obtain the maximum accuracy on all considered meshes.

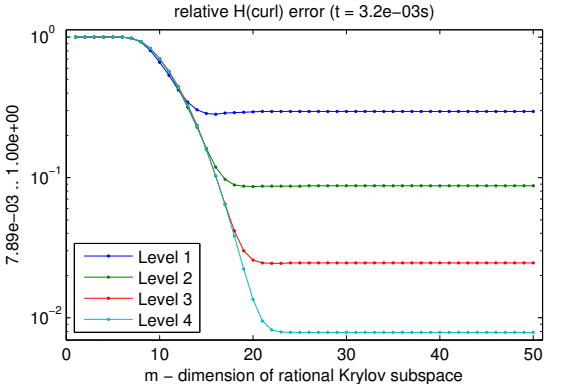

Figure 3. Convergence behavior of the rational Krylov subspace method for fixed time and varying dimension of the subspace. “Level” refers to the different meshes of increasing fineness.

Layered Half-Space with Conductive Structure

The second considered model is a half-space with $\sigma_h = 0.01\,\mathrm{S\,m^{-1}}$ covered by a 100 m thick overburden with $\sigma_o = 0.1\,\mathrm{S\,m^{-1}}$ and an embedded conductive structure with $\sigma_b = 2\,\mathrm{S\,m^{-1}}$. The modeled domain has an extent of 553 m × 553 m × 276 m. A cut of the corresponding mesh on the coarsest level is shown in Figure 4.

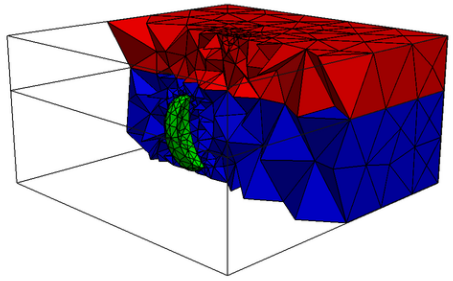

Figure 4. Cut of the coarsest mesh of the layered half-space model with conductive structure. The overburden is shown in red, the underlying half-space in blue and the herein embedded conductive structure in green.

A solution for an exemplary time is plotted in Figure 5.

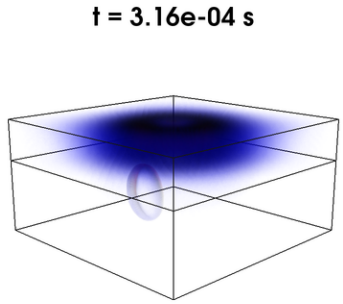

Figure 5. Normalized current densities of the layered half-space model with conductive structure at $t \approx 3.2 \times 10^{-4}$ s. One can nicely see that the conductive structure starts to "capture" the electric currents.

The computation times are similar to the homogeneous half-space model.

CONCLUSIONS

We were able to leverage several state-of-the-art techniques to create a combined efficient forward modeling code that is significantly faster than traditional codes.

ACKNOWLEDGMENTS

We are grateful to the German Research Foundation (DFG) for supporting this research work (Spi 356-9). The author also wishes to thank Jens Seidel for the original implementation of geometric multigrid for Nédélec elements, Ingolf Busch for help with implementing the nonlocal boundary condition, and Stefan Güttel for developing the time integrator using rational Krylov subspaces.

REFERENCES

Arnold, D. N., Falk, R. S., & Winther, R. (2000). Multigrid in H(div) and H(curl). *Numer. Math. 85*, 197–217.

Goldman, Y., Hubans, C., Nicoletis, S., & Spitz, S. (1986, July). A finite-element solution for the transient electromagnetic response of an arbitrary two-dimensional resistivity distribution. *Geophysics*, *51*(7), 1450–1461.

Goldman, Y., Joly, P., & Kern, M. (1989). The Electric Field in the Conductive Half Space as a Model in Mining and Petroleum Prospecting. *Math. Method. Appl. Sci. 11*, 373–401.

Güttel, S. (2010). *Rational Krylov Methods for Operator Functions* (Doctoral dissertation, TU Bergakademie Freiberg).

Oristaglio, M. L. & Hohmann, G. W. (1984, July). Diffusion of Electromagnetic Fields into a Two-Dimensional Earth: A Finite-Difference Approach. *Geophysics*, *49*(7), 870–894.

Wang, T. & Hohmann, G. W. (1993). A Finite-Difference, Time-Domain Solution for Three-Dimensional Electromagnetic Modeling. *Geophysics*, *58*(6), 797–809.

Yee, K. S. (1966). Numerical Solution of Initial Boundary Problems Involving Maxwell's Equations in Isotropic Media. *IEEE Trans. Ant. Propag. 14*, 302–309.